Drop processes in natural clouds

J. Latham

Physics Department, University of Manchester Institute of Science and Technology
PO Box 88, Sackville Street, Manchester M60 1Qd, ENGLAND

Abstract

Water drops are formed at cloud base by condensation upon nuclei and as they rise they grow by vapour diffusion in the slightly supersaturated environment of the clouds. Turbulent mixing between cloudy air and undersatured air entrained from outside produces fluctuations in supersaturation, not linked to changes in vertical velocity, which cause broadening of the condensate spectrum and the rapid production of droplets large enough to engage in growth by coalescence. The probabilities of permanent union or the production of satellite droplets following the collision of a pair of raindrops is a sensitive function of several parameters. In some circumstances electrohydrodynamic bursting may influence the the properties of clouds.

1. Introduction

Liquid drops produced by natural processes in the Earth's atmosphere vary in size from around 0.1um to 1cm — a range of about twelve orders of magnitude in volume. Thus it is not surprising that such drops are involved in a large number of physical processes and phenomena; some of which are of crucial importance to large-scale energy transport, the cleanliness of the atmosphere and the fertility of cultivated land. It would be beyond the scope of this short article to attempt a detailed review of each of these processes. Instead, they are treated, in Section 3, in a cursory manner which, it is hoped, will permit their range and their interdependence to be outlined; and one process - the diffusive mixing of dry and cloudy air, which is considered to be fundamental to the development of natural clouds - is selected for more comprehensive discussion , in the following section. This particular topic has been chosen in view of recent concentration of attention upon it by several groups of scientists.

2. The diffusive mixing of dry air with a population of cloud droplets

The sub-adiabatic liquid-water-contents generally observed within clouds from which ice is absent - or present only in insignificant quantities - are a consequence of the dilution of the clouds, during their growth, with environmental, undersaturated air. Recent work (Baker and Latham, 1979[1]; Baker, Corbin and Latham, 1980[2]; Telford and Chai, 1980[3]; Telford and Wagner, 1981[4]) has indicated that the non-uniform manner with which the environmental air mixes with the cloud gives rise to fluctuations in supersaturation - not linked to changes in updraught speed - which cause spectral broadening. A small fraction of the droplets move through the condensate spectrum to the coalescence stage of growth several times faster than predicted by classical descriptions of the entrainment process (for example, Warner (1973)[5]; Mason and Jonas, (1974)[6]; Lee and Pruppacher (1977)[7]), in which the mixing between environmental and cloudy air at any level was assumed to be instantaneous and uniform. The droplet spectra predicted by Baker et al agreed well with those measured in cumulus by Warner (1969)[8].

Baker et al did not specify the nature of the entrainment process but assumed that a volume of environmental air mixing instantaneously with cloudy air at a given level reduced the droplet population there by means of a combination of dilution and total evaporation of a fraction of droplets of all sizes. Telford and Chai assumed that outside air entrained into the cloud at its top became negatively buoyant as a result of droplet evaporation, and then descended, as a saturated stream, to mix with and thereby dilute cloud air at a lower level. The common consequence of both these mixing processes is a droplet spectrum identical in shape to that prior to mixing, but with reduced number concentrations in all size categories. Subsequent ascent of the mixed volume produces an enhancement in supersaturation as a consequence of reduced competition for water vapour; as a result, the droplets grow more rapidly than those in adiabatic regions of the cloud.

In neither of these studies was account taken of the finite rates at which cloudy and environmental air (or adjacent regions of cloud, with different properties) will mix. In this paper we present a model of the turbulent mixing of a spherical blob of droplet-free air, of original diameter λ_B, temperature T_B and supersaturation S (≤ 0), and a cloud, represented by a spherical shell surrounding the blob of outer diameter λ_C, temperature T_C, supersaturation S ($=0$) and liquid water content L. The blob contains a distribution $n(m_s)$ of cloud condensation nuclei, comprised of NaCl particles of mass m_s in equilibrium at the

relative humidity H = S +1. This distribution is identical to that assumed to be contained within the droplets in the surrounding cloud, so that when turbulent mixing occurs at any level the total concentration of particles (droplets plus CCN) remains constant. The entire system is assumed to be moving upwards with a speed W.

The turbulent mixing of all properties transported is represented by diffusion with a single coefficient K determined on dimensional grounds from λ_B and ϵ, the rate of dissipation of turbulent energy within the cloud: $K = (\lambda_B^4 \epsilon)^{\frac{1}{3}}$. If we assume that the turbulent motions transport energy, liquid-water, water-vapour and dry air simultaneously, we have

$$\frac{\partial h(\underline{R},t)}{\partial t} + W\frac{\partial h(\underline{R},t)}{\partial z} - K\nabla^2 h(\underline{R},t) = Q_h(\underline{R},t), \tag{1}$$

$$\frac{\partial \rho_l(\underline{R},t)}{\partial t} + W\frac{\partial \rho_l(R,t)}{\partial z} - K\nabla^2 \rho_l(\underline{R},t) = Q_l(\underline{R},t), \tag{2}$$

$$\frac{\partial \rho_v(\underline{R},t)}{\partial t} + W\frac{\partial \rho_v(\underline{R},t)}{\partial z} - k\nabla^2 \rho_v(\underline{R},t) = Q_v(\underline{R},t) \tag{3}$$

$$\frac{\partial \rho_a(\underline{R},t)}{\partial t} + W\frac{\partial \rho_a(\underline{R},t)}{\partial z} - k\nabla^2 \rho_a(\underline{R},t) = Q_a(\underline{R},t) \tag{4}$$

$$\frac{\partial n(r_i,\underline{R},t)}{\partial t} + W\frac{\partial n(r_i,\underline{R},t)}{\partial z} - k\nabla^2 n(r_i,\underline{R},t) = Q_n(r_i,\underline{R},t)\,. \tag{5}$$

ρ_a, ρ_l and ρ_v are the densities of dry air, liquid water and water vapour, respectively; $n(r_i, \underline{R}, t)$ is the number density of droplets with radii in the interval (r_i, r_i+dr_i); and $\underline{R}$ is the radial vector. The energy term

$$h = [C_a\rho_a + C_l(\rho_l + \rho_v)]T + \rho_v L_v\,, \tag{6}$$

where C_a and C_l are the specific heat of dry air and liquid water respectively and $L_v (=2.26 \text{KJ g}^{-1})$ is an average value of the latent heat of vapourization of water. Equation (6) defines the temperature T in terms of the parameters of the problem.

The source terms Q are:

$$Q_h(\underline{R},t) = -[L_v Q_v(\underline{R},t) + \rho_a(\underline{R},t)gW(t)] \tag{7}$$

$$Q_v(\underline{R},t) = -4\pi\rho_w \Sigma_i n(r_i,\underline{R},t) r_i^2 \dot{r}_i(\underline{R},t) \tag{8}$$

$$Q_l(\underline{R},t) = -Q_v(\underline{R},t) \tag{9}$$

$$Q_n(r_i,\underline{R},t) = \frac{n(r_i,\underline{R},t)}{\rho_a(\underline{R},t)} \cdot Q_a(\underline{R},t) \tag{10}$$

$$Q_a(\underline{R},t) = -\rho_a(\underline{R},t)\cdot\left[\frac{Q_T(\underline{R},t)}{T(\underline{R},t)} + \frac{gW(t)}{R_a T(\underline{R},t)}\right] \tag{11}$$

where ρ_a is the density of liquid water, g the acceleration due to gravity and R_a the gas constant per kilogramme of air.

$$Q_T(\underline{R},t) = \frac{Q_h(\underline{R},t)}{[C_a\rho_a(\underline{R},t) + C_l(\rho_l(\underline{R},t) + \rho_v(\underline{R},t))]} \tag{12}$$

The droplet growth equation is

$$\dot{r}_i(\underline{R},t) = \frac{D\rho_a(T)/\rho_w}{(r_i+a)}\left[S(\underline{R},t) - \frac{A}{r_i} + \frac{Bm_a}{r_i^3}\right] \tag{13}$$

where

$$\rho_a(\underline{R},t) = 1.8 \times 10^9 \exp(-5400/T(\underline{R},t)) \tag{14}$$

is the saturation vapour density (g m^{-3}), D is the coefficient of molecular diffusion ($cm^2 s^{-1}$), the supersaturation S is expressed as a percentage, r_i is measured in micrometres, m_a in grammes, and the constants A and B possess the values 0.115 and 1.4×10^{13} respectively. a(=5um) is a characteristic length associated with the non-ideality in water condensation.

The rate of change of supersaturation

$$\dot{s}(\underline{R},t) = (100 + s(\underline{R},t))\left[\frac{Q_v(\underline{R},t)}{\rho_v(\underline{R},t)} - \frac{5.4 \times 10^3 Q_T(\underline{R},t)}{T^2(\underline{R},t)} - \frac{3.42 \times 10^{-2} W(t)}{T(\underline{R},t)}\right] \quad (15)$$

The precision of the foregoing equations could be increased, but such refinements were deemed unnecessary, in view of the very approximate relationship between this diffusion formulation and the mixing process within clouds. We note that the diffusivity representation is best applied to situations in which λ_B exceeds the characteristic spatial scale of the turbulent eddies. Although buoyancy gradients generated by evaporation will deform the volume under examination, we assume that spherical symmetry is preserved during the mixing process.

Figure (1) illustrates the predicted time variation of the fields of liquid-water-content, L, supersaturation, S, and temperature, T, resulting from the mixing of a blob of air of size λ_B = 100m and relative humidity 80% with a cloud of size λ_c = 200m and liquid water content L = 0.5g m^{-3}, W = 0 m s^{-1}. In the first case illustrated (A,B,C) the cloud consists of droplets of radius 3um and in the second (D,E,F), r = 20um. Since the turbulent energy dissipation rate $\epsilon = 10^{-2} m^2 s^{-3}$ the characteristic mixing times

$$\tau_{TC} = (\lambda_c^2/\epsilon)^{\frac{1}{3}} = 160s \quad (16)$$

$$\tau_{TB} = (\lambda_B^2/\epsilon)^{\frac{1}{3}} = 100s \quad (17)$$

We see, when r = 3um, that evaporation of droplets carried by turbulence into the interior of the blob is a very rapid process - presumably because of the high surface/volume ratio of the droplets - so that the supersaturation rises from -20% to close on 0% in about 10s. The temperature difference (originally 2K) follows a similar pattern - since its changes are governed by evaporation when the latter is rapid - lagging just slightly behind the changes in S. Evaporation is confined more-or-less entirely to the region originally occupied by the blob. The liquid-water-content distribution takes considerably longer to level out, because evaporation inhibits its increase in the early stages of mixing, but nevertheless the gradient has been substantially reduced after 20 seconds, a period much less than the turbulent mixing times τ_{TC} and τ_{TB}.

Figure 1 shows that when the cloud consists of larger drops (r = 20um) the rate of increase of minimum supersaturation S towards zero is reduced - because evaporation is less effective - but is still essentially completed within 20 seconds. The temperature equalization curves again follow those of S, and there is a corresponding increase in the rapidity with which the gradient in L levels out. In this case turbulence distributed the undersaturation significantly into the cloud. Mixing is largely completed after 20s.

Figure (2) shows the time-development of the initially monodisperse spectrum (r=20um; the droplet concentration N = 15 cm^{-3}; L = 0.5g m^{-3}) at R = $\lambda_B/2$, the location of the original interface between the cloudy and undersaturated air (H = 80%), W = 0.0m s^{-1}. It is seen that the combination of evaporation and turbulent mixing introduces many new categories into the droplet size distribution.

Figure (3) presents the calculated spatial fields of L and S, at various times, for two different values of ϵ, the turbulent energy dissipation rate, W = 0 m s^{-1}. In this case the original spectrum, illustrated (A) in Figure 5, has a liquid water content L = 1.0g m^{-3}. It contains ten size classes (radii between 3 and 12.5um) and is based on ones encountered in field studies on the summit of Great Dun Fell (Blyth et al (1980)[9]). In this case λ_{TC} ~ 130s when $\epsilon = 10^{-2} m^2 s^{-3}$ (A,B) and λ_{TC} ~ 270s when $\epsilon = 10^{-3} m^2 s^{-3}$ (C,D); the corresponding values of λ_{TB} are 74s and 160s. When the mixing is rapid (A,B) the supersaturation becomes uniformly distributed within 20s, and gradients in L are eliminated well before 50s. With slower mixing the equalization of both L and S are slower, but are completed in times less than τ_{TC}. In both cases undersaturations are created within the region occupied by the original cloud; a characteristic feature of the situations in which the cloud spectrum contains large drops - with correspondingly high values of evaporation time τ_r (Baker et al,(1980)[2]).

In figure 4 we present, for the cases covered by Figures 1 and 3, information on the rates at which the total amount of evaporation and the distribution of liquid water approach their final values. f(in curves A,B,C,D) is the ratio of the total evaporation that has occurred at time t(expressed, in Figure 4 as the dimensionless time t/τ_c) to that which has occurred when the cloud and blob are fully mixed. In curves E,F,G,H

$$f = 1 - \frac{(L_c - L_o)_t}{(L_c - L_o)_{t=0}} = 1 - \Delta L/L \qquad (18)$$

where $\Delta L = (L_c - L_o)_t$ is the difference, at time t, between the liquid water contents in the centre of the original blob (R=0) and at the edge of the cloud ($R=\lambda_c/2$); L is the original liquid-water-content in the cloud.

The curves displayed in Figure 4 show clearly that: evaporation is completed long before the gradients in L are eliminated; uniformity in L is achieved - generally - in times much less than τ_{TC}; evaporation proceeds most effectively when droplets are small and mixing is fast. Further calculations (not illustrated) show that uniformity in S is achieved more quickly for increased values of L.

In Figure 5 we present various spectra resulting from the mixing with undersaturated air of a volume of cloud possessing an original liquid-water-content $L = 0.5g\ m^{-3}$ and the size distribution (A) mentioned earlier, $W = 0.0\ m\ s^{-1}$. For the particular dimensions chosen ($\lambda_c = 144m$, $\lambda_B = 60m$) the final - well-mixed - value of L, if the humidity of the entrained air is 70% and the temperatures are as indicated, is $0.32g\ m^{-3}$. Curve B presents the classical spectrum, with $L = 0.32g\ m^{-3}$, which was obtained by the application of the droplet growth equation to all droplets in the original spectrum. All droplets have evaporated, so the peak radius has shifted substantially (whereas the peak concentration is virtually unchanged) and the reduction in radius is greater for the smaller droplets. Curve C, $L = 0.32g\ m^{-3}$, is obtained from our diffusive model, with $\epsilon = 10^{-3}m^2s^{-3}$. This spectrum is seen to have a peak-radius only slightly below that of the original spectrum (A), but a substantially reduced peak-concentration. Thus the spectrum C, predicted from our model, lies between the classical spectrum B and the extreme inhomogeneous spectrum, but is very much closer to the latter - which is not shown since its similarity to B would cause confusion in presentation.

In Figure 6 we present three spectra resulting from the turbulent mixing of spectrum A - the same as in Figure 5 - with a blob of undersaturated air, $W = 0\ \ m\ s^{-1}$. The dimensions and temperatures, given in the legend, are the same for all three calculations. In B and C the reletive humidity H = 70% and the final water content $L = 0.32\ g\ m^{-3}$. In B, $\epsilon = 10^{-3}m^2s^{-3}$ and in C, $\epsilon = 10^{-2}m^2s^{-3}$. Curves B and C are very similar, but B is more 'inhomogeneous' - smaller reduction in peak radius - consistent with the associated slower mixing in this case. Curve D ($L = 0.18g\ m^{-3}$) was obtained with H = 40% and $\epsilon = 10^{-3}m^2s^{-3}$. This spectrum, although very different from one predicted by the classical description of mixing/evaporation (see, for example, Figure 4, Curve B), is substantially different from the equivalent 'extreme inhomogeneous' or 'dilution only' spectrum (again not shown), in which the shape of curve A would be preserved, and the mean radius would be the same as in A. This large departure from the extreme inhomogeneous spectrum may be attributed to the greater role of evaporation (relative to dilution) in producing the final spectrum (D).

In Figure 7 we show the effect of doubling the radius of all droplets in the spectrum A illustrated in Figure 5 and 6, whilst maintaining the liquid water content $L = 0.5g\ m^{-3}$, $W = 0\ \ g\ m^{-3}$. The final spectrum (C) after evaporation and mixing is closer to the classical one B than in the earlier cases, presumably because for these large droplets the ratio of evaporation to mixing times, τ_r/τ_T, (Baker et al (1980)[2]) is no longer much less than unity.

In Figure 8 we attempt to examine, for a wide range of original conditions, the extent to which spectral changes resulting from turbulent mixing of undersaturated and cloudy air conform to the classical (homogeneous) picture or to the alternative extreme discussed by Telford and Chai, and by Baker et al. For ease of interpretation, these calculations were made with originally monodisperse spectra.

On the classical picture, to a first approximation, the concentration of droplets, N, in an originally monodisperse spectrum, is unchanged from the original value N_o, as entrainment reduces the liquid water content from L_o to L. On the extreme inhomogeneous picture, N is reduced in proportion to the reduction in L, (ie $N = (L/L_o)N_o$). On the classical picture the water content is reduced in proportion to the reduction in the radius r(ie $r^3 = (L/L_o)r_o^3$, where r_o is the original radius). On the extreme inhomogeneous picture r is unchanged as L decreases. Thus we may define a parameter

$$\Phi = (N/N_o)(L/L_o)/(R/R_o)^3 \qquad (19)$$

which possesses a value $\Phi = 1$ for all L/L_o on the classicel description of mixing and is given by $\Phi = (L/L_o)^2$ in the extreme inhomogeneous case.

These two extreme curves are plotted in Figure 8, together with individual values of Φ emanating from a variety of calculations, using the diffusive mixing model.

The most important result is that, for all situations considered, the extreme inhomogeneous description of turbulent entrainment provides a much better approximation to reality than does the classical description . The departures from $(L/L_a)^4$ can be quite substantial, however. We see from Figure 8 that this departure increases with: decreasing λ_a, increasing H (at constant L/L_a); decreasing L; decreasing ϵ; and (proportionately), decreasing L/L_a. All these tendencies are consistent with the basic ideas, advanced by Baker et al, that (1) the time constant ratio τ_E/τ_T, which equals zero in the extreme inhomogeneous case, increases with decreasing values of L and λ and with increasing ϵ and H; and (2) that as (L/L_a) is reduced (by reducing H) the contribution of dilution to the overall reduction in water content is reduced.

3. Other processes

It is inappropriate, in an article of this limited length, to do other than to list further important processes, occuring in clouds, which involve drops. For a comprehensive and authoritative treatment of these the reader is referred to the excellent book of Pruppacher and Klett (1978)[10]. The processes include: condensation via heterogeneous nucleation; collision; coalescence; satellite drop production; electrohydrodynamic bursting; mechanical disruption; scavenging of particulate and gaseous pollutants; supercooling; freezing; accretion; secondary ice particle production; splashing; and lightning initiation by corona.

Acknowledgements

Dr M B Baker, of the University of Washington, Seattle, USA, played the primary role in the development of the diffusive mixing model described herein. The special contribution of Dr M Guery is gratefully acknowledged.

References

1. Baker M B & Latham J "The evolution of droplet spectra and the rate of production of embryonic raindrops in small cumulus clouds" J Atmos Sci, Vol 36, pp 1612-1615. 1979
2. Baker M B, Corbin R G & Latham J "The influence of entrainment on the evolution of cloud droplet spectra: I. A model of inhomogeneous mixing", Q J Roy Met Soc, Vol 106, pp 581-598. 1980
3. Telford J W & Wagner P B "Observations of condensation growth not determined by nuclei but by entity type mixing" (Preprint). 1981
4. Telford J W & Chai G K "A new aspect of condensation theory", PAGEOPH, Vol 118, pp 720 742. 1980
5. Warner J "The microstructure of cumulus cloud. PtIV, The effect on the droplet spectrum of mixing between cloud and environment", J Atmos Sci, Vol 30, pp 256-261. 1973
6. Mason B J & Jonas P R "The evolution of droplet spectra and large droplets by condensation in cumulus clouds", Q J Roy Met Soc, Vol 100, pp 23-38. 1974
7. Lee I Y & Pruppacher H R, "A comparative study of the growth of cloud drops by condensation using an air parcel model with and without entrainment", PAGEOPH, Vol 115, pp 523-545. 1977
8. Warner J, "The microstructure of cumulus cloud. Pt 1, General features of the droplet spectrum", J Atmos Sci, Vol 26, pp 1049-1059. 1969.
9. Blyth A M, Choularton T W, Fullarton G, Latham J, Mill C S, Smith M H & Stromberg I M, "The influence of entrainment on the evolution of cloud droplet spectra: II. Field experiments at Great Dun Fell", Q J Roy Met Soc, Vol 106, pp 821-840. 1980.
10. Pruppacher H R & Klett J D, Microphysics of Clouds and Precipitation, D Reidel (1978)

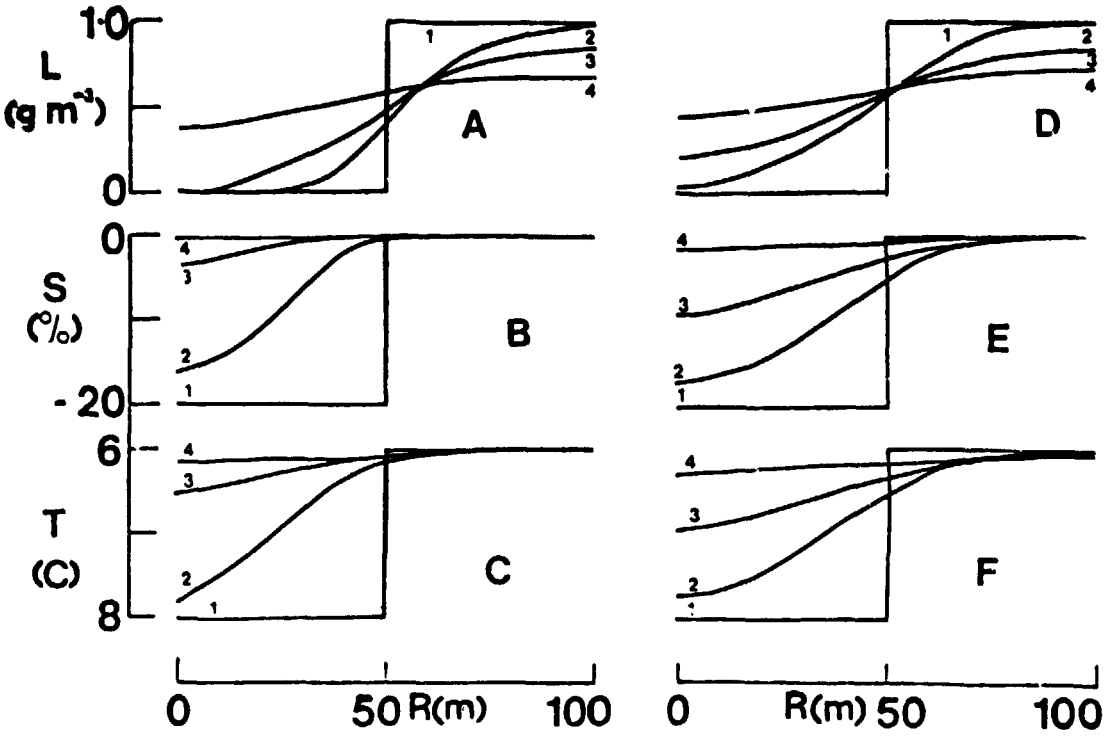

Figure 1: Calculated radial distributions of liquid-water-content, L, supersaturation S and temperature T at various times t during the turbulent mixing of a water cloud with a spherical blob of undersaturated air centrally embedded within it at t=0. Single category spectra. λ_b=100m;λ_c=200m;$\epsilon=10^{-2}m^2s^{-3}$;$m_s=10^{-16}$g;L=1.0g m^{-3};H=80%; T_B=281K;T_c=279K.A,B,C:r=3um;D,E,F:r=20um. 1, t=0;2, t=5s;3, t=10s;4 t=20s.

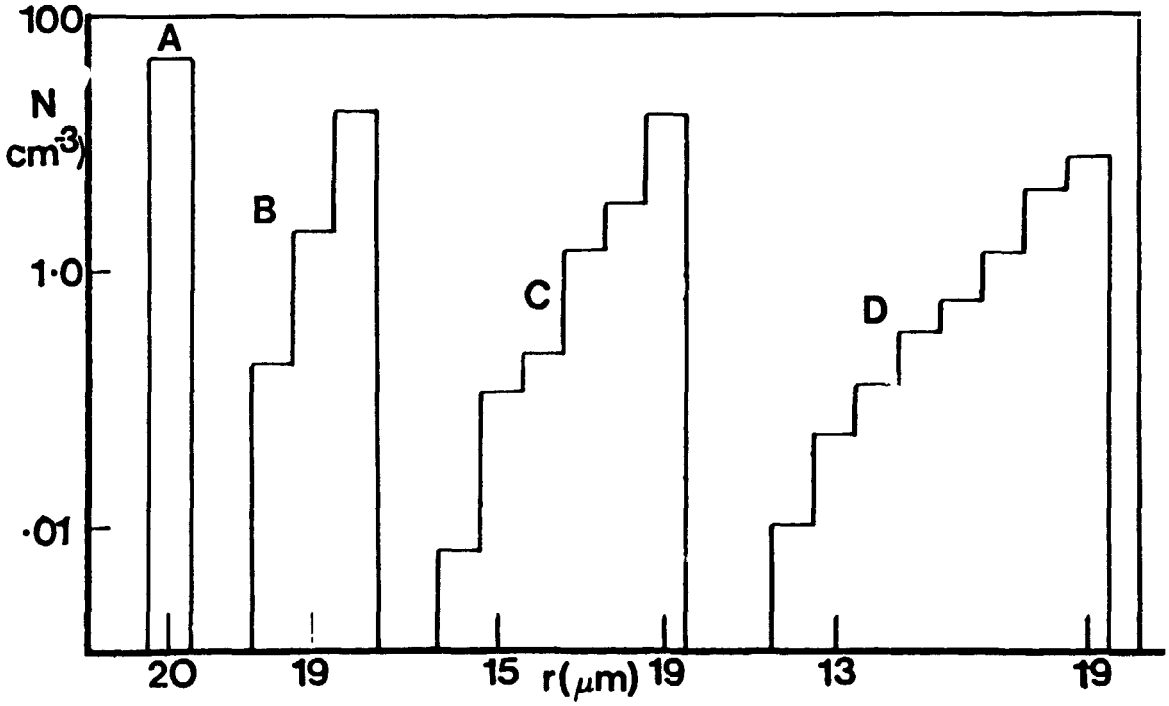

Figure 2:Calculated drop-size spectra at $R=\lambda_B/2$ at various times t during the turbulent mixing of a water cloud with a spherical blob of undersaturated air centrally embedded within it at t=0. Singel category spectrum. r=20um;λ_B=100m;λ_c=200m;$\epsilon=10^{-2}m^2s^{-3}$;H=80% T_B=281K;T_c=279k.A,t=0; B, t=5s; C, t=10.2s; D, t=12s.

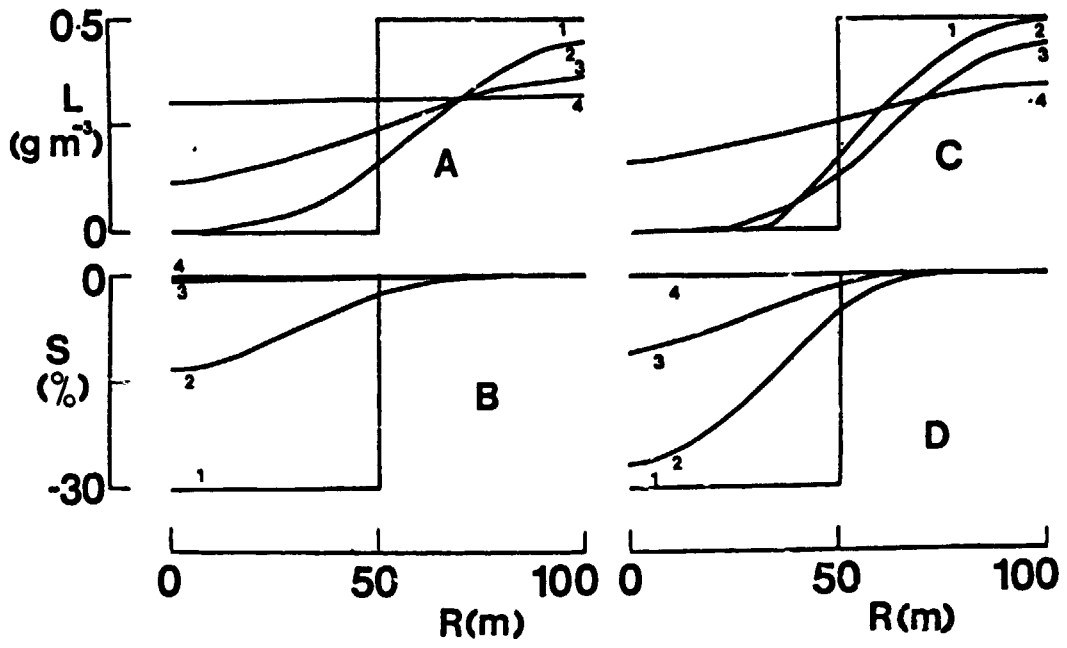

Figure 3: Calculated radial distributions of liquid-water-content, L, and supersaturation S at various times t during turbulent mixing of a water cloud with a spherical blob of undersaturated air centrally embedded within it at t=0. Ten category spectrum. λ_B = 60m; λ_C =144m; $m_s = 10^{-16}$g; L = 1.0g m^{-3}; H = 70%; T_B= 281k; T_C= 279K. A, B, $\epsilon = 10^{-2} m^2 s^{-3}$; C, D, $\epsilon = 10^{-3} m^2 s^{-3}$;.
1, t = 0.0s; 2, t= 8s; 3, t = 20s; 4, t = 50s.

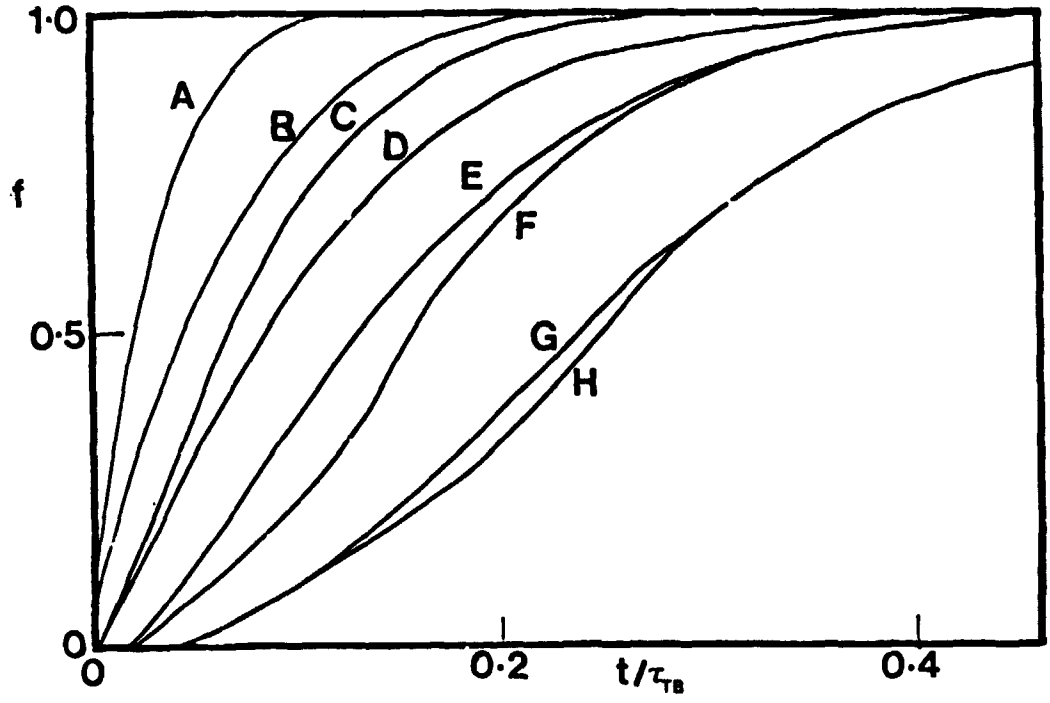

Figure 4: Calculated variation with dimensionless time t/τ_{TB} of the parameter f (defined in the text) which governs the rate at which the evaporative process and the redistribution of liuqid water occurs, during the turbulent mixing of a water cloud with a spherical blob of undersaturated air centrally embedded within it. at $t/\tau_{TB} = 0$; $m_s=10^{-16}$m; T_B=218k; T_c= 279K; l+1.0g m^{-3}.
Curves A, D, E, F are for a single category spectrum, r = 3um; (A,F), r=20μm (D,E).
Curves B, C, G, H are for the 10-category spectrum (Figure 2). Curves A, B, C, D are for the evaporation; Curves E, F, G, H for liquid water (eqn 23).
Curves A, D, E, F: λ_B = 60m; λ_c = 200m; $\epsilon = 10^{-2}m^2s^{-3}$; H=70%.
Curves B, G λ_B=60m; λ_c= 144m; $\epsilon = 10^{-3}m^2s^{-3}$; H = 70%.

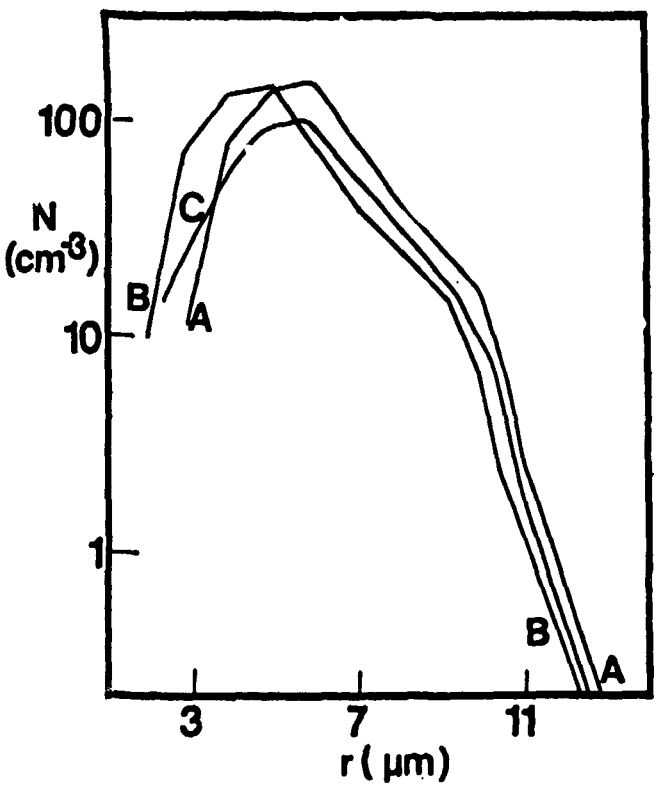

Figure 5: Droplet size distribution (C) calculated by application of the diffusive model to the mixing of a spherical blob of undersaturated air with a water cloud possessing the size distribution (A) at time t = 0. Spectrum B is calculated on the classical model of mixing. The liquid water content in A is 0.5g m^{-3} and in B and C 0.32g m^{-3}. λ_B = 60m; λ_C = 144m; $\epsilon = 10^{-3} m^2 s^{-3}$; H = 70%; T_B=281K; T_C= 279K; $m_s = 10^{-18}$g.

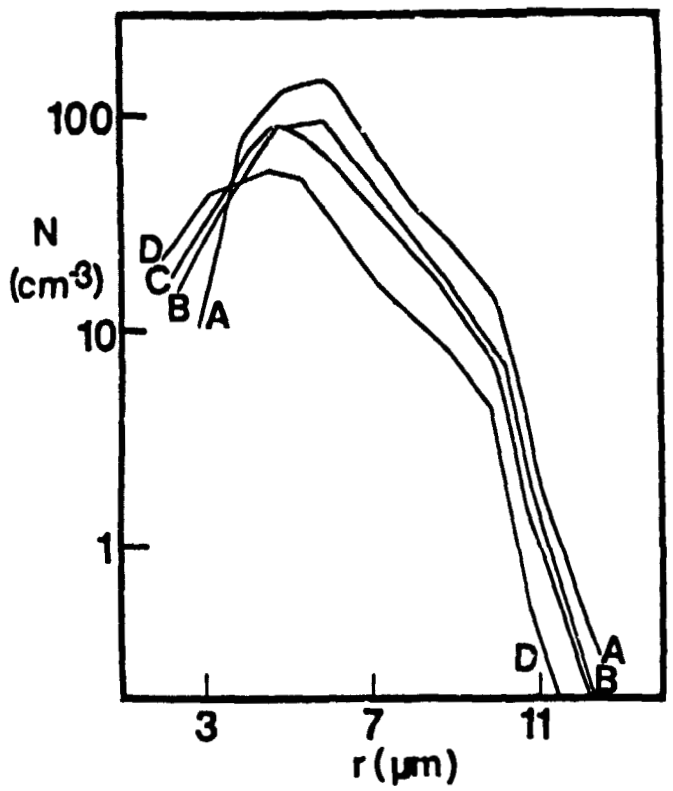

Figure 6: Droplet size distributions (B), (C) and (D) calculated by application of the diffusive model to the mixing of a spherical blon of undersaturated air with a water cloud possessing the size distribution (A) at time t=0. λ_B=60m; λ_C=144m; T_B= 281K; T_C=279K; $m_s=10^{-16}$g; L=0.5g m^{-3}; B, $\epsilon=10^{-3}m^2s^{-3}$, H=70%; C, $\epsilon=10^{-2}m^2s^{-3}$; H=70%; D, $\epsilon=10^{-3}m^2s^{-3}$.

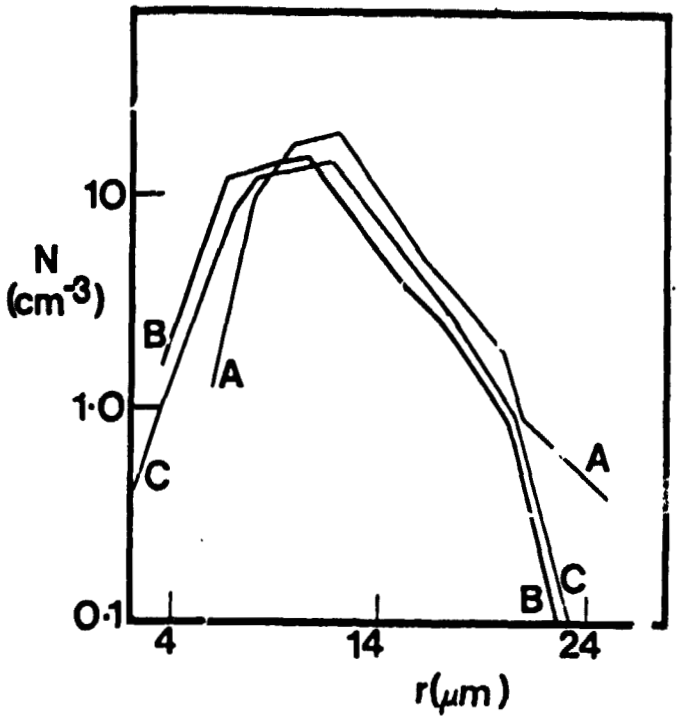

Figure 7: Droplet size distribution (C) calculated by application of the diffusive model to the mixing of a spherical blob of undersaturatd air with a water cloud possessing the size distribution (A) at time t = 0. Spectrum (B) is calculated on the classical model of mixing. The liquid water content in A is 0.5g m^{-3} and and in B and C 0.32g m^{-3}. λ_B= 60 m; λ_C= 144m; ϵ= $10^{-2}m^2s^{-3}$; H = 70% T_B=281K; T_C=279K; m_s=10^{-16}g.

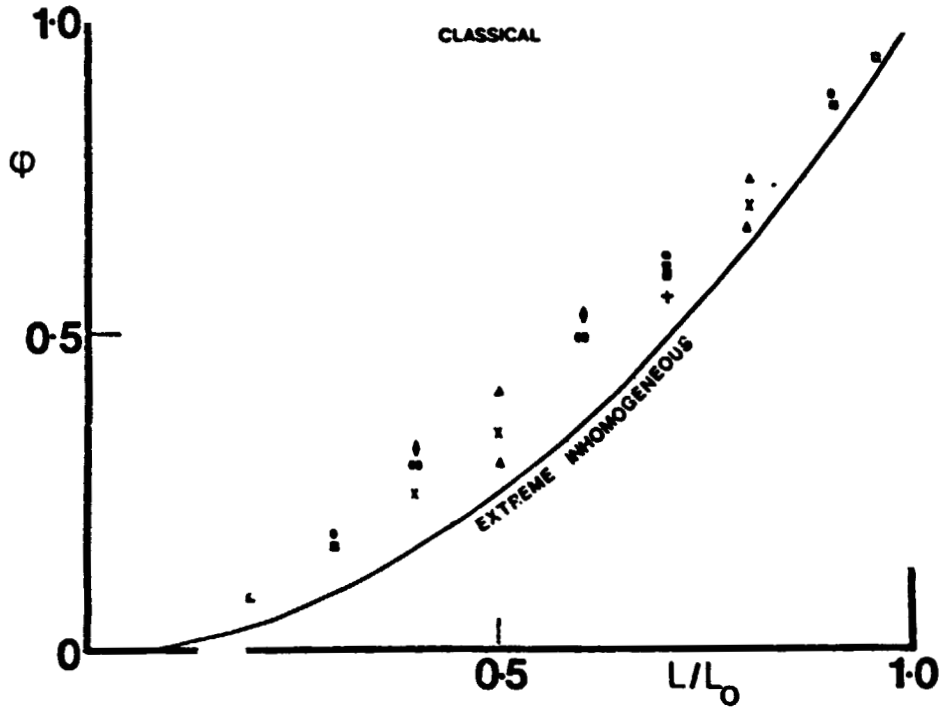

Figure 8: Values of the parameter Φ, defined by equatio (24), calculated from the diffusive mixing model for various values of L/L_o and permutations of other parameters. Single category spectra. Except where indicated λ_B= 100m; λ_c=400m; r = 10um; T_B= 281k; T_c=279K; $m_s=10^{-16}$g; H= 80%; $\epsilon= 10^{-2}m^2s^{-3}$; L= 1.0g m^{-3}. This permutation provides points (M).
(●), L=0.5g m^{-3}; ▲, λ_B=20m, λ_c=80m;
x, λ_B=30m; λ_c=120m; Δ, λ_B=200m, λ_c=800m;
, r=30um; , r=20um; +, $\epsilon= 10^{-3}m^2s^{-3}$;
, H=70%, , H=40%